Effects of Solvents on Adsorption Energies: a General Bond-Additivity Model

James Akinola[1,2], Charles T. Campbell[3*], Nirala Singh[1,2*]
[1]Department of Chemical Engineering, and [2]Catalysis Science and Technology Institute
University of Michigan
Ann Arbor, Michigan 48109-2136, USA
[3]Department of Chemistry
University of Washington
Seattle, Washington 98105-1700, USA

ABSTRACT

While a vast body of knowledge exists about adsorption energies of catalytic reaction intermediates on solid surfaces in gas or vacuum conditions based on experimental studies and calculations using quantum mechanics, much less is known about adsorption energies in the presence of liquid solvents. We present here a method for estimating adsorption energies in liquid phase based on the gas-phase adsorption energy, the solvent's adhesion energy to the solid surface and the gas-phase adsorbate's solvation energy. A simple bond-additivity model was recently developed for approximating the change in adsorption energy (relative to gas phase) due to the additional presence of liquid solvents using the solvent's adhesion energy and the gaseous adsorbate's solvation energy, but that model was limited to adsorbates whose thickness is much smaller than its lateral dimension (parallel to the surface). Here we present a simple extension of that model to adsorbates of finite thickness and general shape. We propose a model to convert the experimental solvation energy of a gaseous molecule into a molecule-solvent adhesion energy by assuming isotropic interaction of the molecule with the solvent. This adhesion energy allows us to estimate the fraction of this solvation energy that is retained when the molecule is adsorbed, based on the molecule's shape, size, and adsorption geometry. As in the earlier bond-additivity model, adsorption energies in solvent are lower in magnitude than in the gas phase by an amount approximately equal to the adhesion energy of the solvent to the surface times the surface area of the solvent molecules displaced upon adsorption. We also report the predicted effects of different solvents for molecules on metal surfaces where solvation energies, gas-phase adsorption energies and solvent / surface adhesion energies are available in the literature.

* Corresponding authors: charliec@uw.edu and snirala@umich.edu

INTRODUCTION

Understanding the adsorption energetics of molecules on solid surfaces in liquid solvents is important for improving catalytic and electrocatalytic reactions such as used in fuel production and combustion, fuel cells, biomass conversions, catalytic methane and CO_2 conversions, plastics upcycling, and environmental remediation. The increasing importance of these reactions on solid surfaces in liquid phase, for example in catalytic biomass conversions and in electrochemical storage of renewable energy, requires an improved understanding of the effect of solvents on adsorption. The solvent is well known to strongly influence catalytic activity and selectivity.[1–13] The reasons for this are still not well understood, but certainly derive from the effect of the solvent on the energies of adsorbed reaction intermediates and elementary-step transition states. Adsorption energies on solid surfaces in liquid phase also play a large role in controlling corrosion, whose annual costs are in the hundreds of billions of dollars.[14]

Learning how to transfer current knowledge of the energetics of reactions at gas/solid interfaces to liquid/solid interfaces would be extremely valuable due to the vast knowledge of reactions at gas/solid interfaces and methods for studying them compared to liquid/solid interfaces. Particularly important would be to develop methods for estimating the effect of liquid solvents on the energies of adsorbed reaction intermediates and transition states in catalytic and electrocatalytic reaction mechanisms, as this would facilitate the development of microkinetic models for estimating reaction kinetics that have been so fruitful in gas-phase catalysis research, but sorely lacking for reactions in liquid solutions. There have been numerous studies to compare heats of adsorption measured in liquid solvents with those in the gas phase[15–18] and to use simulations to clarify the role of the solvent.[1,2,12,16,18–20] There are several reviews and viewpoints that discuss the challenges involved in modeling solvent effects.[21,22] Generally, modeling efforts to speed up computational work incorporating solvent effects include implicit modeling of the solvent as a homogeneous constant dielectric continuum, bilayer adsorption (ice model), explicit modeling of the solvent by inclusion of solvent molecules in the simulation, and mixtures of implicit and explicit solvation.[21–25] Examples of implicit models are the conductor-like screening model (COSMO[26]) which uses an approximation of the solvent as a dielectric continuum with a cavity for the molecule.[27,28] Explicit models may make use of molecular dynamics and density functional theory (DFT).[29,30] Explicit hybrid quantum-mechanical/molecular mechanics (QM/MM) have been used to capture the effect for phenol on Pt(111) in water.[31]

We have recently shown how a simple bond-additivity model can be employed to estimate adsorption energies in the liquid phase for "flat" neutral molecules using measured gas phase adsorption energies and the adhesion energy of the solvent to the solid, explaining the difference in aqueous-phase and gas-phase adsorption energies for phenol and benzene on Pt(111).[32,33] This model built upon the concept from Gileadi[34] and Bockris and Jeng[15] to account for the displacement of solvent at the interface, but incorporated important additional solvent-solvent and solvent-adsorbate interactions. This model showed that solvent/solid adhesion energies are critical in understanding solvent effects on adsorption energies. We therefore subsequently also reported experimental adhesion energies for a range of solvents on Pt(111) and Ni(111).[33] Using this bond-additivity method together with some experimental data mentioned above allowed

predictions of aqueous adsorption energies for several adsorbates on Pt and Rh surfaces from simple gas-phase DFT calculations, with reasonable agreement with experimental results.[35]

In this work, we extend that simple bond-additivity model for flat molecules[32] to adsorbates of finite thickness and arbitrary shape. We derive an equation that allows one to estimate the adsorption energy in liquid solvents for a reactant molecule of arbitrary shape based on five values that are known or can be measured or estimated with reasonable accuracy: (1) the molecule's gas-phase adsorption energy, (2) the adhesion energy of the solvent to the solid surface, (3) the area on the surface where solvent molecules are blocked by the adsorbate, (4) the total "surface area" of the solvent cavity that must be created to solvate the free reactant molecule, and (5) the reactant's solvation energy (relative to the free gas-phase molecule), which can be derived from the temperature dependence of its Henry's law constant. This opens up many opportunities for predicting solvent effects on adsorption energies and, from that, solvent effects on catalytic reaction rates.

We show that the adsorption energy in solvent is smaller in magnitude than in gas phase by an amount approximately equal to the adhesion energy of the solvent to the solid times the area of the surface where solvent molecules are displaced upon reactant adsorption.

RESULTS AND DISCUSSION

Bond-additivity model for molecules of finite thickness

In **Figure 1**, we show a diagram of the individual steps involved in the adsorption of a reactant molecule, R, onto a solid surface, M, in the presence of solvent, S. This model is similar to the bond-additivity model proposed previously,[32,33] but here accounts for adsorbates of finite thickness. The original model was for uncharged adsorbates like benzene and phenol that lie flat on the surfaces of metals like Pt(111) and Rh(111), whose thickness is very small compared to the dimension parallel to the surface. The total outer surface area of such adsorbates (σ_{tot}) is approximately just the area of the top and bottom of the molecule. We extend that model here to the more general case for uncharged adsorbates of arbitrary thickness, to now include the sides of the molecule in estimating the energies of these steps. **Figure 1** applies only to low coverages of the adsorbate, so that these sides contact solvent molecules rather than other adsorbates, and any adsorbate-adsorbate interactions are neglected here.

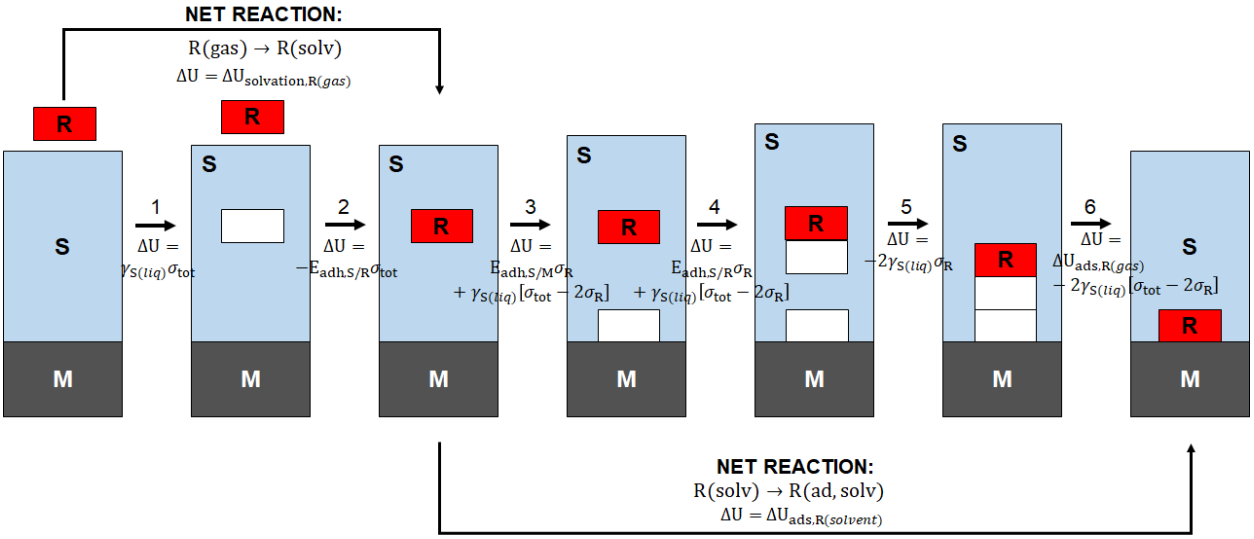

Figure 1. Thermodynamic cycle to determine the energy of adsorption of a reactant molecule (R) with finite thickness onto a solid surface (M) in a condensed-phase solvent (S) from its energy of adsorption in the gas-phase. Each numbered step's change in internal energy (ΔU) is indicated. The gas-phase adsorption energy is denoted $\Delta U_{ads,R(gas)}$. The solvent surface energy ($\gamma_{S(liq)}$) and adhesion energy of the solvent onto the surface ($E_{adh,S/M}$) and of the solvent onto the molecule ($E_{adh,S/R}$) are energies per unit area. They are multiplied by areas of either the footprint of the molecule on the surface (σ_R), in the particular adsorbed configuration of interest, or the total outer surface of the molecule (σ_{tot}).

Solvation energy

The first two steps depicted in **Figure 1** consist of solvation of the gas-phase reactant (R). First a cavity or void volume is created in the solvent (S) with the volume and shape required for the reactant molecule (Step 1), giving an internal energy penalty equal to the surface energy of the solvent ($\gamma_{S(liq)}$) multiplied by the total outer surface area associated with the newly formed cavity (σ_{tot}). This is analogous to the use of a solvent cavity for computation of solvation energies as previously reported.[36,37] Then, as the gas-phase R is moved into this cavity (Step 2), there is a favorable energy equal to the interaction energy per unit surface area between the solvent and the reactant ($E_{adh,S/R}$) multiplied by σ_{tot}. We use the term adhesion energy to refer to $E_{adh,S/R}$ due to its conceptual similarity to the commonly-known "adhesion energy" between any two surfaces of condensed phases, which is generally accepted to mean the attractive interaction energy per unit area between the two surfaces, starting with them in vacuum and well separated (as used here also). The net energy of these two steps is equal to the solvation energy of the molecule, which is tabulated and readily available for many molecules:

$$\Delta U_{solvation,R(gas)} = \gamma_{S(liq)}\sigma_{tot} - E_{adh,S/R}\sigma_{tot} \quad (1)$$

This allows us to determine the adhesion energy per surface area between the solvent and the reactant, $E_{adh,S/R}$, if the outer surface area of the reactant is known:

$$\mathrm{E_{adh,S/R}} = \frac{-\Delta \mathrm{U_{solvation,R}}(gas)}{\sigma_{\mathrm{tot}}} + \gamma_{\mathrm{S}}(liq) \quad \textbf{(2)}$$

The outer area could be estimated, for example, from the molecular geometry (gas-phase structure) by smoothly connecting the outer van der Waals radii of the outer atoms. We show other methods for estimating σ_{tot} below. **Eq. 2** assumes that the interaction energy per unit area between the reactant molecule and solvent molecules is uniform around this outer surface area of the molecule, i.e., isotropic.

For flat adsorbates that are only one atom thick, like benzene and phenol[32,33], we previously assumed they are infinitely thin as a reasonable approximation. In that limit, the total surface area is just the surface area of the top and bottom of the molecule (both equal to the footprint area of the molecule, σ_{R}). In that limit, this interaction energy in **Eq. 2** reduces to:

$$\mathrm{E_{adh,S/R}} = \frac{-\Delta \mathrm{U_{solvation,R}}(gas)}{2\sigma_{\mathrm{R}}} + \gamma_{\mathrm{S}}(liq) \quad \textbf{(3)}$$

This matches the result we derived previously for such a shape.[33] To make this more clear, we rearrange this and use the definition of S-R from that previous work[33] to give:

$$\mathrm{E_{adh,S/R}}\sigma_{\mathrm{R}} \equiv \text{S-R} = \frac{-\Delta \mathrm{U_{solvation,R}}(gas)}{2} + \gamma_{\mathrm{S}}(liq)\sigma_{\mathrm{R}} \quad \textbf{(4)}$$

In an example case of a square molecule that is not flat, but instead has a thickness that is ¼ of its side length (such that $\sigma_{\mathrm{tot}} = 3\sigma_{\mathrm{R}}$), **Eq. 2** gives:

$$\mathrm{E_{adh,S/R}} = \frac{-\Delta \mathrm{U_{solvation,R}}(gas)}{3\sigma_{\mathrm{R}}} + \gamma_{\mathrm{S}}(liq) \quad \textbf{(5)}$$

Adsorption energy of solvated reactant molecule

We now analyze the energies of a set of elementary steps which combine to result in the adsorption of this solvated molecule onto the solid surface, and thus has a net energy equal to its adsorption energy with both the unbound and adsorbed reactant in liquid solution, $\Delta \mathrm{U_{ads,R}}(solvent)$. Once the molecule is solvated, another cavity must be formed, but instead of in the bulk solution, this cavity is at the surface of the solid (M) (Step 3). The energy of this cavity formation includes the energies to remove solvent from some of the solid surface and to create gas/solvent surfaces around the edges of this cavity. The first contribution is reverse (negative) of the adhesion energy of the solvent to the solid surface ($\mathrm{E_{adh,S/M}}$) multiplied by the area of the adsorbate footprint (σ_{R}). Note that this is a different adhesion energy than between the solvent and the adsorbate and instead of the total surface area, only the footprint area is used. The second contribution is the energy penalty of breaking solvent-solvent bonds to make solvent/gas surface (which costs $\mathrm{E_{adh,S/R}}$ per unit area created), but only for the area of the cavity touching the solvent that is not touching the solid surface, i.e., only the "sides" of the cavity, $\sigma_{\mathrm{tot}} - 2\sigma_{\mathrm{R}}$. (Creating the top surface of the cavity is included in the definition of $\mathrm{E_{adh,S/M}}$ above, so is not included here.) We use a value for $\mathrm{E_{adh,S/R}}$ here determined from the experimental solvation

energy as described above in **Eq. 2**. The combined energy for Step 3 is thus $\Delta U_3 = E_{adh,S/M}\sigma_R + \gamma_{S(liq)}[\sigma_{tot} - 2\sigma_R]$.

In Step 4, another cavity is formed just below the solvated adsorbate, again of the same size and shape as the molecule. This energy penalty is similar to that of the cavity formed at the surface, with a solvent/molecule adhesion energy $E_{adh,S/R}$ (determined from the solvation energy as described above), multiplied by the footprint of the cavity plus the surface energy of the solvent multiplied by the area of the "sides" of the cavity: $\Delta U_4 = E_{adh,S/R}\sigma_R + \gamma_{S(liq)}[\sigma_{tot} - 2\sigma_R]$.

In Step 5, these two cavities in the solvent are combined, with the favorable energy from decreasing the solvent/gas surface area (twice σ_R because two interfaces are removed: the top of the cavity on the solid surface and the bottom of the cavity under the adsorbate) times the surface energy of the solvent: $\Delta U_5 = -2\gamma_{S(liq)}\sigma_R$.

The final step (Step 6) is adsorption of the molecule, which is downhill in energy due to the bonding of the molecule to the solid surface and the removal of solvent/gas surface area. In this simple bond-additivity model, we assume that the bond energy of the molecule to the solid surface equals the energy of adsorption of that molecule in the gas-phase, $\Delta U_{ads,R(gas)}$, and is unaffected by the presence of the solvent on the other surfaces of the molecule. The removal of solvent/gas surface area along the cavity "sides" is downhill in energy by $2\gamma_{S(liq)}[\sigma_{tot} - 2\sigma_R]$. The combined energy for Step 6 thus equals $\Delta U_6 = \Delta U_{ads,R(gas)} - 2\gamma_{S(liq)}[\sigma_{tot} - 2\sigma_R]$.

Thus, the overall adsorption energy of the solvated molecule R (Steps 3-6) equals the sum of these steps' energies:

$$\Delta U_{ads,R(solvent)} = E_{adh,\frac{S}{M}}\sigma_R + \gamma_{S(liq)}[\sigma_{tot} - 2\sigma_R] + E_{adh,\frac{S}{R}}\sigma_R + \gamma_{S(liq)}[\sigma_{tot} - 2\sigma_R] - 2\gamma_{S(liq)}\sigma_R + \Delta U_{ads,R(gas)} - 2\gamma_{S(liq)}[\sigma_{tot} - 2\sigma_R] \quad \textbf{(6)}$$

The contributions from the solvent surface energy associated with the sides of the molecules cancel here, so this simplifies to:

$$\Delta U_{ads,R(solvent)} = E_{adh,S/M}\sigma_R + E_{adh,S/R}\sigma_R - 2\gamma_{S(liq)}\sigma_R + \Delta U_{ads,R(gas)} = \Delta U_{ads,R(gas)} + \left[E_{adh,S/M} + E_{adh,S/R} - 2\gamma_{S(liq)}\right]\sigma_R \quad \textbf{(7)}$$

This is the same equation as we obtained for a flat molecule previously.[33] However, a difference arises when we substitute for $E_{adh,S/R}$ here our equation above for $E_{adh,S/R}$ in terms of the molecule's experimental solvation energy (**Eq. 2**). That gives:

$$\Delta U_{ads,R(solvent)} = \Delta U_{ads,R(gas)} + \left[E_{adh,S/M} + \left(\frac{-\Delta U_{solvation,R(gas)}}{\sigma_{tot}} + \gamma_{S(liq)}\right) - 2\gamma_{S(liq)}\right]\sigma_R \quad \textbf{(8)}$$

This can be rearranged to obtain the adsorption energy in solvent as a function of the gas-phase adsorption energy, the adhesion energy of the solvent to the surface, the solvation energy of the adsorbate, the surface energy of the solvent, and the footprint and total area of the molecule:

$$\Delta U_{ads,R(solvent)} = \Delta U_{ads,R(gas)} + \left[E_{adh,S/M} - \frac{\Delta U_{solvation,R(gas)}}{\sigma_{tot}} - \gamma_{S(liq)}\right]\sigma_R \quad \textbf{(9)}$$

For the simple case of a "flat adsorbate" as discussed above, $\sigma_{tot} = 2\sigma_R$, and **Eq. 9** simplifies to:

$$\Delta U_{ads,R(solvent)} = \Delta U_{ads,R(gas)} + E_{adh,S/M}\sigma_R - \frac{\Delta U_{solvation,R(gas)}}{2} - \gamma_{S(liq)}\sigma_R \quad \textbf{(10)}$$

This is the same as we previously obtained.[33]

When the total area is instead three times that of the footprint:

$$\Delta U_{ads,R(solvent)} = \Delta U_{ads,R(gas)} + E_{adh,S/M}\sigma_R - \frac{\Delta U_{solvation,R(gas)}}{3} - \gamma_{S(liq)}\sigma_R \quad \textbf{(11)}$$

Reactant molecule of non-rectangular shape

Here we show that the equations derived above (i.e., **Eq. 2** to determine $E_{adh,S/R}$ and **Eq. 9** to determine $\Delta U_{ads,R(solvent)}$) also apply to molecules that do not have 'sides' that are perpendicular to the top and bottom. For example, in **Figure 2** we show a case where the 'top' of the molecule has a different area ($\sigma_{R,top}$) than the 'footprint' of the molecule on the solid surface (σ_R). Here, the solvation of the molecule (Steps 1 plus 2) is the same as for **Figure 1**, so the solvation energy and **Eq. 2** are unchanged. Just as with **Figure 1**, **Figure 2** applies only to low coverages of the adsorbate, so that the sides of the adsorbate contact solvent molecules rather than other adsorbates, and any adsorbate-adsorbate interactions are neglected here.

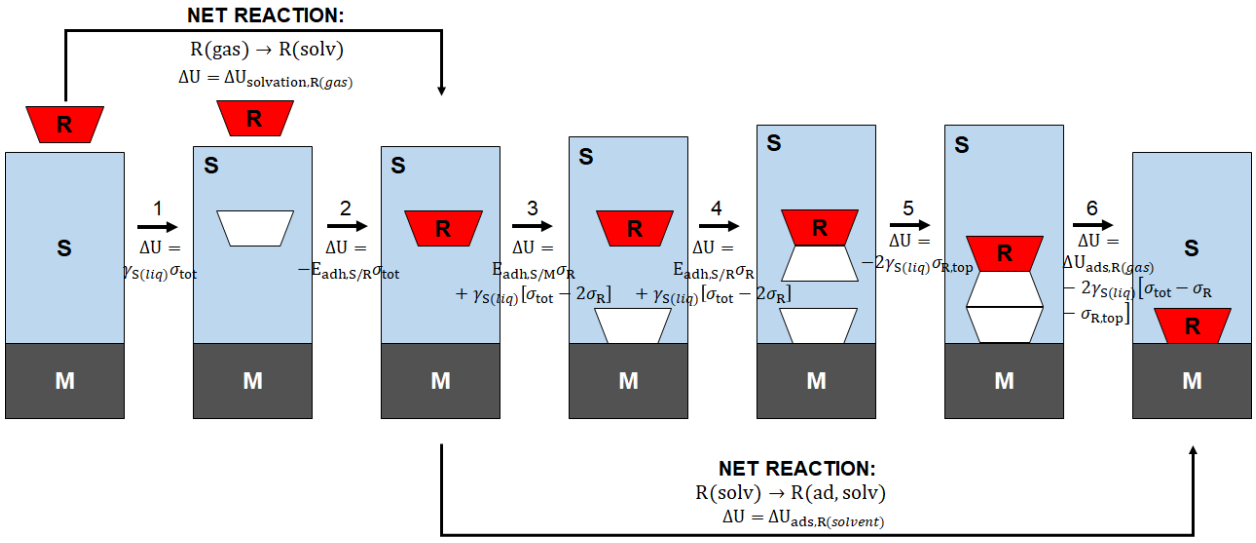

Figure 2. Thermodynamic cycle to determine the energy of adsorption of a reactant molecule (R) with finite thickness onto a solid surface (M) in a condensed-phase solvent (S) from its energy of adsorption in the gas-phase, just as in Figure 1, but now where the reactant has a top area ($\sigma_{\mathrm{R,top}}$) that is different than its footprint area on the surface (σ_{R}).

In Step 3, the energy penalty to create the cavity is still the same as in **Figure 1**: $\Delta \mathrm{U}_3 = \mathrm{E}_{\mathrm{adh,S/M}}\sigma_{\mathrm{R}} + \gamma_{\mathrm{S}(liq)}[\sigma_{\mathrm{tot}} - 2\sigma_{\mathrm{R}}]$.

It is the same because the area of the cavity touching the solvent that is not touching the solid surface is still $\sigma_{\mathrm{tot}} - 2\sigma_{\mathrm{R}}$. (Again, creating a part of the top surface area of the cavity equal to σ_{R} is included in the definition of $\mathrm{E}_{\mathrm{adh,S/M}}$, so is not included here.)

Similarly, in Step 4 a cavity is formed but in this case the adhesion energy is that of the solvent and the molecule: $\Delta \mathrm{U}_4 = \mathrm{E}_{\mathrm{adh,S/R}}\sigma_{\mathrm{R}} + \gamma_{\mathrm{S}(liq)}[\sigma_{\mathrm{tot}} - 2\sigma_{\mathrm{R}}]$, the same as in **Figure 1**. The cavity 'formed' in Step 4 is inverted to include the areas of the new interfaces formed and was simply needed for the derivation, but is not meant to indicate that an actual physical inverted cavity formed during an adsorption process.

Step 5 combines the cavities, where now the interfacial area being removed is that of the "top" of the molecule, $\sigma_{\mathrm{R,top}}$: $\Delta \mathrm{U}_5 = -2\gamma_{\mathrm{S}(liq)}\sigma_{\mathrm{R,top}}$

In the final step, Step 6, the reactant molecule is adsorbed as before, and the interfacial area of the sides of the cavities are removed. The difference here compared to Step 6 in **Figure 1** is that the area of the sides of the molecule is not $\sigma_{\mathrm{tot}} - 2\sigma_{\mathrm{R}}$, but instead $\sigma_{\mathrm{tot}} - \sigma_{\mathrm{R}} - \sigma_{\mathrm{R,top}}$: $\Delta \mathrm{U}_6 = \Delta \mathrm{U}_{\mathrm{ads,R}(gas)} - 2\gamma_{\mathrm{S}(liq)}[\sigma_{\mathrm{tot}} - \sigma_{\mathrm{R}} - \sigma_{\mathrm{R,top}}]$

The adsorption energy of the solvated molecule is the sum of the energies of Steps 3, 4, 5, 6, giving:

$$\Delta U_{ads,R(solvent)} = E_{adh,\frac{S}{M}}\sigma_R + \gamma_{S(liq)}[\sigma_{tot} - 2\sigma_R] + E_{adh,\frac{S}{M}}\sigma_R + \gamma_{S(liq)}[\sigma_{tot} - 2\sigma_R] - 2\gamma_{S(liq)}\sigma_{R,top} + \Delta U_{ads,R(gas)} - 2\gamma_{S(liq)}[\sigma_{tot} - \sigma_R - \sigma_{R,top}] \quad \textbf{(12)}$$

This is analogous to **Eq. 6** above and similar. Through cancellation of terms and rearranging, **Eq. 12** simplifies to again give **Eq. 7**:

$$\Delta U_{ads,R(solvent)} = \Delta U_{ads,R(gas)} + [E_{adh,S/M} + E_{adh,S/R} - 2\gamma_{S(liq)}]\sigma_R \quad \textbf{(7)}$$

This proves that **Eqs. 7** and **9** are completely independent of the shape of the reactant molecule, from a negligibly thin, flat molecule as when originally derived[32] to the more complex, realistic shapes in Figures 1 and 2. It requires knowing the area of contact between the solvent molecules and the solid surface that is blocked upon the reactant's adsorption (σ_R) and the adhesion energies ($E_{adh,S/M}$ and $E_{adh,S/R}$) to relate the reactant's adsorption energy in solvent to that in gas phase.

From **Eq. 7**, **Eq. 9** can be obtained in the same way as above (i.e., using **Eq. 2** to get $E_{adh,S/R}$ from the solvation energy of R(gas), $\Delta U_{solvation,R(gas)}$), to give:

$$\Delta U_{ads,R(solvent)} = \Delta U_{ads,R(gas)} + \left[E_{adh,S/M} - \frac{\Delta U_{solvation,R(gas)}}{\sigma_{tot}} - \gamma_{S(liq)}\right]\sigma_R \quad \textbf{(9)}$$

This equation too is independent of the shape of the molecule except in that the shape determines the ratio σ_R/σ_{tot}. The value of σ_{tot} is not in **Eq. 7**, but it arises here because it was needed in **Eq. 2** to determine $E_{adh,S/R}$ from the solvation energy.

Eq. 9, or **Eqs. 7** and **2**, make a complete picture of the energy difference between adsorption in the gas phase versus adsorption in a liquid phase solvent which is independent of molecule shape (except via the ratio σ_R/σ_{tot}). It assumes pairwise bond-additivity within the special context we introduced in ref. [32] which extends bond energies beyond the usual concept of atom-atom or molecule-molecule bond energies to instead consider the bond energy per unit contact area between substances, i.e., adhesion energies. It requires that the molecule's "surface" is isotropic in its interaction with solvent molecules, as this was assumed in deriving the relationship between $E_{adh,S/R}$ and $\Delta U_{solvation,R(gas)}$ given in **Eq. 2**.

The ratio σ_R/σ_{tot} is dependent on the adsorption configuration on the surface. The application of **Eq. 9**, or **Eqs. 7** and **2** should therefore be for the specific configuration and orientation of interest. This is particularly important for molecules which can adsorb in multiple different configurations or that have coverage-dependent adsorption configurations. The adsorption energy in the gas phase also changes with the adsorbate's configuration / orientation.

Eq. 9 shows that the reactant's adsorption energy in the solvent is smaller in magnitude than in the gas phase by an amount that is proportional to its footprint on the solid (i.e., the area where it blocks solvent molecules from binding to the solid). The proportionality constant ($E_{adh,S/M} - \frac{\Delta U_{solvation,R(gas)}}{\sigma_{tot}} - \gamma_{S(liq)}$) equals the adhesion energy of the solvent to the solid plus

the magnitude of the reactant's solvation energy per unit of reactant total surface area minus the solvent's surface energy. It also can be written as $E_{adh,S/M} + E_{adh,S/R} - 2\gamma_{S(liq)}$. This proportionality constant is dominated by the adhesion energy of the solvent to the solid since the other two terms are smaller and opposite in sign so they nearly cancel (see below). This near cancellation was found also from applications of the original bond-additivity model to relatively flat molecules on Pt and Rh surfaces.[32,35]

Table 1 lists the magnitude of this proportionality constant (in the last column) for various reactant molecules in various solvents adsorbing on the Pt(111) surface near room temperature. Also listed are the molecules' solvation energies, taken from tabulated enthalpies of solvation after converting to energies by adding RT. The value of σ_{tot}, the total surface area of the molecule in contact with the solvent in bulk solution (per mole), is also needed to estimate this proportionality constant. It is estimated here by assuming the molecule's shape, thickness and footprint area on the surface (σ_R per mole) estimated as follows. For benzene, phenol and n-hexane, their maximum coverages when adsorbed on Pt(111) terraces in their most stable structure are known from experimental measurements (equal to 1/9, 1/9 and 1/7 per Pt surface atom, respectively[38–40]). Dividing the area per mole of Pt atoms on Pt(111) (4.02×10^4 m^2/mol) by this maximum coverage gives the footprint area per mole of molecule, σ_R. We then use the known molar volume of the reactant molecule (V_m, calculated from its reported density as a pure bulk liquid) together with this footprint area to estimate the molecule's thickness, t, as $t = V_m / \sigma_R$ for these three reactant molecules. As expected, this gives a thickness which is within a few percent for benzene and phenol (0.247 and 0.251 nm). We then assume this same thickness as with phenol for all of the other aromatic molecules in **Table 1**: t = 0.251 nm. Similarly, we assume that all n-alkanes have the same thickness as estimated in this way for n-hexane: t = 0.465 nm. Given this estimated thickness, the footprint area for each of the other molecules (for which the maximum coverage is not already known from the literature) is then estimated from its molar volume by: $\sigma_R = V_m / t$. The value of σ_{tot} is estimated from σ_R and t by assuming a simplified molecular shape. We assume a thin cylindrical disk shape for: benzene, phenol, toluene, and benzaldehyde; and a shallow rectangular box shape for n-alkanes, naphthalene, acetophenone, and styrene. The box width for all aromatics is assumed to be the same as the width (diameter) of benzene's circular disk shape (0.874 nm). The box length for all n-alkanes is estimated as the distance between the farthest two terminal H atoms in the gas-phase structure (as reported in the NIST's CCBDB database) plus twice the van der Waals radius of H atoms in alkanes (0.11 nm [41]), giving 1.04 and 1.30 nm for n-hexane and n-octane, respectively.

Table 1. Solvation energy, footprint surface area (σ_R), total surface area exposed to solvent in bulk solution (σ_{tot}), solvation energy per unit area, solvent/reactant adhesion energy ($E_{adh,S/R}$), and predicted change in adsorption energy on Pt(111) due to the solvent for reactants in different solvents. Solvent surface energies and adhesion energies to Pt(111) (taken from the literature) are included for each solvent. The numbers in brackets after the values refer to literature citations.

Solvent = water, $\gamma_{S(liq)}$ = 0.073 J/m^2, $E_{adh,S/M}$ for Pt(111) = 0.32 J/m^2 [32,33,d]						
Reactant (R)	$\Delta U_{solvation,R(gas)}$ (kJ/mol)[a]	$\sigma_R \times 10^{-5}$ (m^2/mol)[b]	$\sigma_{tot} \times 10^{-5}$ (m^2/mol)[c]	$\Delta U_{solvation,R(gas)}/\sigma_{tot}$ (J/m^2)	$E_{adh,S/R}$ (J/m^2)	$E_{adh,S/M} + E_{adh,S/R} - 2\gamma_{S(liq)}$ (J/m^2)
Pyridine	−46.5	3.21	12.4	−0.0375	0.111	0.28
Phenol	−47.5	3.61	11.4	−0.0417	0.115	0.29
Benzene	−30.5	3.61	11.3	−0.0270	0.100	0.27
Toluene	−34.5	4.24	13.0	−0.0266	0.100	0.27
n-Hexane	−59.5	2.81	17.0	−0.0349	0.108	0.28
n-Octane	−62.5	3.49	21.2	−0.0294	0.102	0.28
Benzaldehyde	−39.5	4.01	12.4	−0.0318	0.105	0.28
Naphthalene	−27.5	4.48	14.2	−0.0194	0.092	0.27
Styrene	−32.5	4.57	14.4	−0.0226	0.096	0.27
Acetophenone	−47.5	4.66	14.6	−0.0325	0.106	0.28
Solvent = benzene, $\gamma_{S(liq)}$= 0.0288 J/m^2, $E_{adh,S/M}$ for Pt(111) = 0.447 J/m^2 [33]						
Reactant (R)	$\Delta U_{solvation,R(gas)}$ (kJ/mol)	$\sigma_R \times 10^{-5}$ (m^2/mol)	$\sigma_{tot} \times 10^{-5}$ (m^2/mol)	$\Delta U_{solvation,R(gas)}/\sigma_{tot}$ (J/m^2)	$E_{adh,S/R}$ (J/m^2)	$E_{adh,S/M} + E_{adh,S/R} - 2\gamma_{S(liq)}$ (J/m^2)
Phenol	−48.8 [42]	3.61	11.4	−0.0424	0.071	0.46
Solvent = n-hexane, $\gamma_{S(liq)}$= 0.0179 J/m^2, $E_{adh,S/M}$ for Pt(111) = 0.16 J/m^2 [43]						
Reactant (R)	$\Delta U_{solvation,R(gas)}$ (kJ/mol)	$\sigma_R \times 10^{-5}$ (m^2/mol)	$\sigma_{tot} \times 10^{-5}$ (m^2/mol)	$\Delta U_{solvation,R(gas)}/\sigma_{tot}$ (J/m^2)	$E_{adh,S/R}$ (J/m^2)	$E_{adh,S/M} + E_{adh,S/R} - 2\gamma_{S(liq)}$ (J/m^2)
Benzene	−28 [44]	3.61	11.3	−0.0249	0.043	0.17
Solvent = methanol, $\gamma_{S(liq)}$= 0.0225 J/m^2,[45] $E_{adh,S/M}$ for Pt(111) = 0.168 J/m^2 [33]						
Reactant (R)	$\Delta U_{solvation,R(gas)}$ (kJ/mol)	$\sigma_R \times 10^{-5}$ (m^2/mol)	$\sigma_{tot} \times 10^{-5}$ (m^2/mol)	$\Delta U_{solvation,R(gas)}/\sigma_{tot}$ (J/m^2)	$E_{adh,S/R}$ (J/m^2)	$E_{adh,S/M} + E_{adh,S/R} - 2\gamma_{S(liq)}$ (J/m^2)
Benzene	−29 [44]	3.61	11.3	−0.027	0.049	0.17
Toluene	−34 [44]	4.24	13.0	−0.026	0.049	0.17

a. Energies of solvation in water are from the temperature dependence of Henry's law constant listed in the NIST WebBook.

b. The σ_R value is based on experimental measurements for benzene, phenol, and n-hexane, and estimated for other reactants by using its molar volume (from its density as a pure bulk liquid) and assuming its thickness as described in the text.

c. The σ_{tot} value is estimated by assuming the molecule's shape and thickness as described in the text, and the σ_R value from the previous column.

d. The $E_{adh,S/M}$ value for water / Pt(111) is different from ref. 33 versus ref. 32 (0.32 vs. 0.251 J/m^2, where the difference arose from the use of the surface energy of solid water versus liquid water in its calculation from the heats of water adsorption[33]). We use here the value from ref. 32 to be consistent with the calculations in our original paper[32] that introduced this bond additivity model.

Using **Eq. 9** and the values in **Table 1**, one is able to use reported adsorption energies in gas-phase to estimate their adsorption energies in liquid solvents. As examples, we show values estimated in this way for several molecules on Pt(111) and Ni(111) in several solvents in **Table 2**. An example calculation of this type for the specific case of phenol on Pt(111) is described in the following section.

Table 2. Predicted energies of adsorption in solvents estimated from experimental gas-phase heats of adsorption using **Eq. 9** and listed values in **Table 1**. Experimental energies of adsorption in solvents are included where available in the literature.

Molecule (R)	Metal (M)	Solvent (S)	$E_{adh,S/M}$ (J/m^2)[a]	$\Delta U_{ads,R(g)}$ (kJ/mol)[b]	$\sigma_R \times 10^{-5}$ (m^2/mol)	$\Delta U_{ads,R(solvent)}$ (kJ/mol) from bond-additivity	$\Delta U_{ads,R(solvent)}$ (kJ/mol) from experiment
Phenol	Pt(111)	Water	0.32 [32,33,c]	−174 [39]	3.61	−70	−19 [46]
	Pt(111)	Benzene	0.447 [33]	−174 [39]	3.61	−7.7	
	Ni(111)	Water	0.417 [33,c]	−175 [39]	2.91	−62	
	Ni(111)	Benzene	0.60 [33]	−175 [39]	2.91	+5	
Benzene	Pt(111)	Water	0.32 [32,33,c]	−162 [38]	3.61	−63	
	Pt(111)	n-Hexane	0.16 [43]	−162 [38]	3.61	−102	
	Pt(111)	Methanol	0.168 [33]	−162 [38]	3.61	−100	
	Ni(111)	Water	0.417 [33,c]	−168 [38]	2.91	−59	
n-Hexane	Pt(111)	Water	0.32 [32,33,c]	−80 [40]	2.81	−1	

a. Adhesion energy of liquid solvent to this metal surface (apart from water, see footnote c).
b. Standard enthalpies of adsorption (averaged from zero up to the maximum coverage), converted to energies by adding *RT*. We assume that the value is the same at 300 K as the T used in the specified references. Calorimetry measurements were done at $T = 90$ K or 150 K.
c. The $E_{adh,S/M}$ value for water / Pt(111) is different from ref. 33 versus ref. 32 (0.32 vs. 0.251 J/m^2). We use here the value from ref. 32 to be consistent with the calculations in our original paper[32] that introduced this bond additivity model. Consequently, the $E_{adh,S/M}$ value for water / Ni(111) is also different from the value given in ref. 33 (0.345 J/m^2), since we changed it to be consistent with the way it was calculated for Pt(111) in ref. 32.

The only experiment available to compare to these predictions in Table 2 at this stage is phenol on Pt(111) in water. Although the model predicts that the heat of adsorption in water will decrease by 104 kJ/mol compared to the gas phase, the observed decrease is 155 kJ/mol. Most but not all of the solvent effect is captured with this model. As we have noted before,[32] part of this disagreement is probably due to the fact that phenol may be at higher local coverage for this experimental result in water, whereas the gas-phase adsorption energy used here is the average for the first layer, which decreases by over 60 kJ/mol in the first layer.[39] As another source of error, this bond-additivity model assumes that the bond strength between the reactant (phenol) and the surface (Pt(111)) does not change when solvent (water) is added on top of the phenol. It seems this water weakens that bond to some extent. That is not unexpected since this same effect (the weakening of bonds as more neighbors are added) is the well-known weakness of the bond-additivity model for predicting atom-atom bonding energetics within molecules.

Because the effect of the solvent on heats of reactant adsorption is so large, and because most of it is captured with this new model, this model will be useful for predicting trends in how

different solvents affect adsorption energies. It also provides an intuitive approach for understanding and explaining the various contributions to solvent effects.

This method is intended for application to relatively small adsorbates where a substantial fraction of the total molecular area is in contact with the solid surface. It is not likely to be accurate for highly flexible, polyfunctional molecules. It is not intended for adsorbed transition states for elementary surface reaction steps, although if the solvent has a similar effect on the adsorption energies of both the adsorbed reactant and the adsorbed product for an elementary step, it seems reasonable to assume that the transition state might be similarly affected too, unless it has charge separation present in neither reactant nor product.

Although this method enables one to estimate energies, free energies can also be estimated from these by also estimating the entropies of adsorption. This can be done by referencing to a gas phase molecule, using established correlations between the gas phase entropy and the entropy of the adsorbed molecule,[47] as we have done for phenol adsorption on Pt(111) in water.[46]

Case study for effect of adsorbate thickness

As an example of the use of **Eq. 9** to determine how much the adsorption energy changes (compared to the gas-phase value) due to a solvent within this modified bond-additivity model, we consider the specific case of phenol adsorbing onto a Pt(111) surface in water. We compare the case where phenol is assumed to have negligible thickness with the result using the more realistic thickness estimated in **Table 1**.

The phenol molecule was approximated in **Table 1** to have the shape of a thin cylindrical disk for simplicity, as shown in **Figure 3**. The footprint area of phenol (σ_R) is 0.60 nm^2 per phenol or 3.61×10^5 m^2 per mole phenol based on the structure of highest-coverage of adsorbed phenol in its most stable structure on Pt(111), corresponding to a (3x3) overlayer with an absolute coverage of 1/9 per Pt(111) surface atom.[32,48] Note that this footprint corresponds to a radius of r = 4.37×10^{-10} m for a circular area. The molar volume of phenol is $V_m = 0.0000905$ m^3 per mole or 1.50×10^{-28} m^3 per phenol based on its reported density. The thickness of a cylinder that has this volume and footprint is $t = V_m / \sigma_R = 2.51 \times 10^{-10}$ m (2.51 Å). The total outer surface area of that cylinder is $\sigma_{tot} = 2\sigma_R + 2\pi rt = 1.14 \times 10^6$ m^2 per mole, as listed in **Table 1**. Note that this gives that $\sigma_{tot} = 3.16\ \sigma_R$, which is approximately $\sigma_{tot} = 3\ \sigma_R$, such that the surface area of the sides is approximately equal to the surface area of the footprint. We instead used $\sigma_{tot} = 2\ \sigma_R$ when we assumed negligible thickness in our original bond-additivity model.[32]

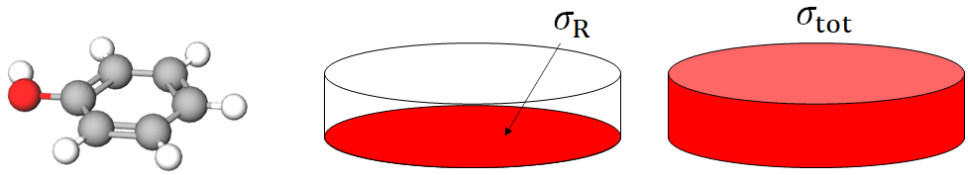

Figure 3. Phenol represented as a uniform molecule with footprint σ_R and total outer surface area σ_{tot}. If phenol is infinitely thin, $\sigma_{tot} = 2\ \sigma_R$. If the thickness (height) of the molecule is 2.51 Å and its footprint area is 0.60 nm^2, as estimated here (see **Table 1**), then $\sigma_{tot} = 3.16\ \sigma_R$.

Note that the shape of the molecule does not have to be a cylinder to apply such an approach as in **Figure 3**, so long as the footprint area and the total surface area can be estimated based on the shape and size.

To solve **Eq. 7**, we need a few values. We will use the reported experimental solvation energy for phenol in water:[32,49] $\Delta U_{solvation,R(gas)} = -47.5\ \text{kJ mol}^{-1}$. The surface energy of liquid water is 0.073 J m^{-2}.[50]

In the case where phenol is assumed to be infinitely thin, we can use **Eq. 3** (that special case of **Eq. 2**) to calculate $E_{adh,S/R}\sigma_R$ in water:

$$E_{adh,\frac{S}{R}}\sigma_R \equiv \text{S-R} = \frac{-(-47.5\ \text{kJ mol}^{-1})}{2} + (0.073\ \text{J m}^{-2})(3.61 \times 10^5\ \text{m}^2\ \text{mol}^{-1}) = 50.1\ \text{kJ mol}^{-1} \quad \textbf{(13)}$$

This is the same as previously reported.[32,33] The value of $E_{adh,S/R}$ is thus (for the infinitely thin molecule):

$$E_{adh,S/R} = \frac{50.1\ \text{kJ mol}^{-1}}{3.61 \times 10^5\ \text{m}^2\ \text{mol}^{-1}} = 0.139\ \text{J m}^{-2} \quad \textbf{(14)}$$

In the case where phenol is not infinitely thin, but instead $\sigma_{tot} = 3.16\ \sigma_R$, we can use **Eq. 5** (that special case of **Eq. 2**) to obtain:

$$E_{adh,S/R} = \frac{-(-47.5\ \text{kJ mol}^{-1})}{3.16(3.61 \times 10^5\ \text{m}^2\ \text{mol}^{-1})} + 0.073\ \text{J m}^{-2} = 0.115\ \text{J m}^{-2} \quad \textbf{(15)}$$

As expected, the interaction (adhesion) of the phenol to the water solvent on an area basis is lower than with the completely flat phenol, because of the higher surface area that we are considering for the phenol. Using the average calorimetric gas-phase adsorption energy of phenol on Pt(111) from zero to maximum coverage:[39]

$$\Delta U_{ads,R(gas)} = -174\ \text{kJ mol}^{-1} \quad \textbf{(16)}$$

The adsorption energy in the limit of low coverage is stronger, but it increases (weakens) by at least 50 kJ/mol in the first layer. (We argued previously that hydrophobic effects may drive phenol to reach higher local coverage when in water, even when its average coverage is very

low.[32]) Thus, here and in **Table 2** we use the average energy. The adhesion energy of water to Pt(111) is:[32,51,52]

$$\mathrm{E_{adh,S/M}} = 0.32\ \mathrm{J\ m^{-2}} \quad \textbf{(17)}$$

The adsorption energy of phenol in water assuming an infinitely flat molecule can be calculated from **Eq. 9**, using the gas-phase adsorption energy of phenol and the other above values:

$$\begin{aligned}\Delta \mathrm{U_{ads,R}}(solvent) &= \Delta \mathrm{U_{ads,R}}(gas) + \left[\mathrm{E_{adh,\frac{S}{M}}} - \frac{\Delta \mathrm{U_{solvation,R}}(gas)}{\sigma_{\mathrm{tot}}} - \gamma_{\mathrm{S}(liq)}\right]\sigma_{\mathrm{R}} \\ &= (-174\ \mathrm{kJ\ mol^{-1}}) \\ &+ \left[0.32\ \mathrm{J\ m^{-2}} - \frac{-47.5\ \mathrm{kJ\ mol^{-1}}}{7.22 \times 10^5\ \mathrm{m^2\ mol^{-1}}} - (0.073\ \mathrm{J\ m^{-2}})\right](3.61 \times 10^5\ \mathrm{m^2\ mol^{-1}}) \\ &= -61\ \mathrm{kJ\ mol^{-1}}\end{aligned} \quad \textbf{(18)}$$

For the case where phenol is not infinitely thin, but instead $\sigma_{\mathrm{tot}} = 3.16\ \sigma_{\mathrm{R}}$, the adsorption energy of phenol in water can again be calculated from **Eq. 9**.

$$\begin{aligned}\Delta \mathrm{U_{ads,R}}(solvent) &= \Delta \mathrm{U_{ads,R}}(gas) + \left[\mathrm{E_{adh,\frac{S}{M}}} - \frac{\Delta \mathrm{U_{solvation,R}}(gas)}{\sigma_{\mathrm{tot}}} - \gamma_{\mathrm{S}(liq)}\right]\sigma_{\mathrm{R}} \\ &= (-174\ \mathrm{kJ\ mol^{-1}}) \\ &+ \left[0.32\ \mathrm{J\ m^{-2}} - \frac{-47.5\ \mathrm{kJ\ mol^{-1}}}{1.14 \times 10^6\ \mathrm{m^2\ mol^{-1}}} - (0.073\ \mathrm{J\ m^{-2}})\right](3.61 \times 10^5\ \mathrm{m^2\ mol^{-1}}) \\ &= -70\ \mathrm{kJ\ mol^{-1}}\end{aligned} \quad \textbf{(19)}$$

Note that in both of these models for phenol's structure, the difference in adsorption energy in solvent versus gas phase is dominated by $\mathrm{E_{adh,S/M}}\sigma_{\mathrm{R}}$ (and approximately equal to this). Here when using $\sigma_{\mathrm{tot}} = 3.16\ \sigma_{\mathrm{R}}$, the adsorption energy is ~9 kJ/mol (~15%) more negative (stronger) than in the infinitely-thin approximation ($\sigma_{\mathrm{tot}} = 2\ \sigma_{\mathrm{R}}$) because the phenol is retaining more of its bonding to water when (properly) assuming that its sides are also exposed to the water after adsorption. Essentially, if $\sigma_{\mathrm{tot}} = 2\ \sigma_{\mathrm{R}}$, when the phenol is adsorbed, only half of it remains "solvated", the top surface. This means there is a larger penalty when adsorbing in the aqueous-phase. When we assume $\sigma_{\mathrm{tot}} = 3.16\ \sigma_{\mathrm{R}}$, ~2/3 of the phenol remains "solvated", the top surface and the sides (which we assume to be the same area as the surface and bottom of the phenol molecule).

We plot the predicted adsorption energy of phenol in water as a function of $\sigma_{\mathrm{R}}/\sigma_{\mathrm{tot}}$ in **Figure 4** using **Eq. 7**. As this ratio increases (i.e., more solvation is lost upon adsorption), the adsorption energy in solvent is weakened, but this change is minor compared to the difference between the gas-phase and aqueous-phase adsorption energy. Note that when changing the value of $\sigma_{\mathrm{R}}/\sigma_{\mathrm{tot}}$, σ_{R} is being held constant at its experimental value.

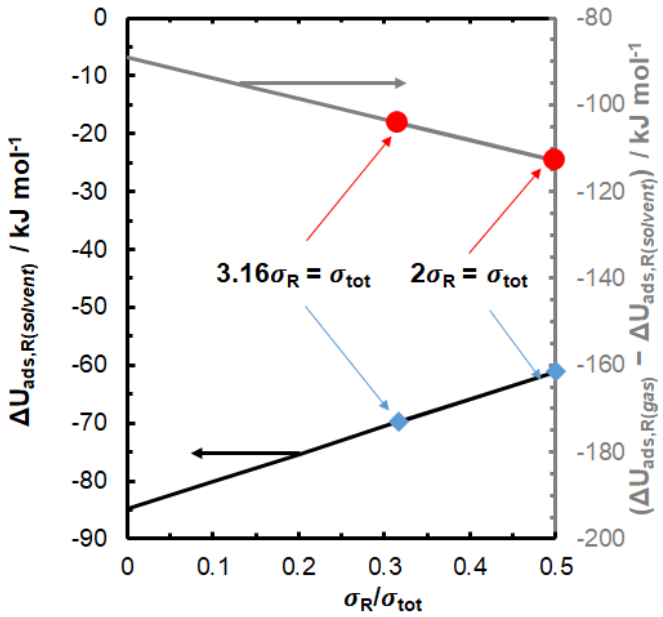

Figure 4. Energy of adsorption of phenol onto Pt(111) in water at 298 K as a function of the ratio of the footprint of phenol on the Pt surface to the total surface area of phenol, calculated using Eq. 7. The ratio of the footprint of phenol to the total surface area is essentially the fraction of solvation of the molecule that is lost due to adsorption. The right-hand axis shows the calculated difference in adsorption energy between gas phase and aqueous phase. For phenol on Pt(111) as described in the text: $\sigma_R = 3.61 \times 10^5$ m^2 mol^{-1}, $E_{adh,S/M} = 0.32$ J m^{-2}, $\Delta U_{solvation,R(gas)} = -47.5$ kJ mol^{-1}, $\gamma_{S(liq)} = 0.073$ J m^{-2}, and $\Delta U_{ads,R(gas)} = -174$ kJ mol^{-1}.

Solvation energies per unit molecular area, and organic / solvent adhesion energies

The negative of the solvation energy per unit molecular area ($-\Delta U_{solvation,R(gas)}/\sigma_{tot}$) listed for organic molecules in **Table 1** equals the adhesion energy at the solvent/organic interface minus the surface energy of the solvent ($E_{adh,S/R} - \gamma_{S(liq)}$). It is important to note that this value is quite similar for all the aromatic molecules in water (~0.02 to 0.03 J/m^2) except for the one that has an OH group (phenol), which is ~0.01 J/m^2 larger, presumably due to its ability to hydrogen bond with water. After adding to these values the surface energy of water (0.073 J/m^2), we see in **Table 1** that the water/organic adhesion energies ($E_{adh,S/R}$) are ~0.092 to 0.100 J/m^2 for all the aromatics unless they contain an oxygen, for which $E_{adh,S/R}$ is ~0.105 and 0.115 J/m^2 for =C=O and –OH groups, respectively. These values for oxygen-free aromatics are similar to but ~35% larger than those found from contact angle measurements for bulk liquid/liquid adhesion energies.[53] Larger adhesion energies than bulk values are expected for such small objects, at least based on measurements of metal nanoparticle adhesion to oxide surfaces.[54] The $E_{adh,S/R}$ values for the alkanes/water in **Table 1** are also quite similar. Adhesion energies in **Table 1** for aromatics to benzene are ~30% smaller than to water, and ~50% smaller for aromatics to n-hexane and methanol than to water. The physically reasonable values for $E_{adh,S/R}$ found in this

way in **Table 1** lend credence to the assumptions used above in the derivation of **Eq. 9**. Since the values are so similar for similar classes of molecules, they also allow estimations to be made of solvent effects for other species not listed in **Tables 1** and **2**. One can imagine using such differences in $E_{adh,S/R}$ values for different classes of adsorbates to further refine the model by breaking down the total surface area of the adsorbate into different parts, for which different $E_{adh,S/R}$ values would be applied.

CONCLUSIONS

We recently developed a bond-additivity model one can use to estimate adsorption energies of "flat" molecules in liquid solvents using the experimental gas-phase adsorption energy of the molecule to the surface, the solvent's adhesion energy to the surface, as well as the energy of solvation of the gas molecule, and showed that it provides moderate accuracy compared to experiments and enables predictions in important trends.[32] In this present work, we show that this model can be extended to molecules that are not infinitely flat but have larger thickness by assuming the interaction between the reactant molecule and solvent molecules is isotropic, and using the geometry of the molecule to estimate the fraction of its "solvation area" that is retained upon adsorption. This modified model allows application of the bond-additivity model to a wider variety of adsorbates of interest for catalysis and electrocatalysis. According to this model, the adsorption energy in solvent can be predicted from the adsorption energy in gas phase using **Eq. 9**:

$$\Delta U_{ads,R(solvent)} = \Delta U_{ads,R(gas)} + \left[E_{adh,S/M} - \frac{\Delta U_{solvation,R(gas)}}{\sigma_{tot}} - \gamma_{S(liq)}\right]\sigma_R \quad \textbf{(9)}$$

As seen, the two adsorption energies differ by an amount proportional to the footprint area of the molecule on the surface, with a proportionality constant that is dominated by the adhesion energy of the solvent to the surface, with smaller and nearly cancelling contributions from the molecule's solvation energy per unit molecular area and the solvents surface energy. This equation is independent of the shape of the molecule except in that the shape determines σ_R and the ratio σ_R/σ_{tot}. It reduces to the equation from our original bond-additivity model for molecules (like phenol and benzene) which were assumed to have negligible thickness (i.e., where $\sigma_{tot} = 2\ \sigma_R$, by simply replacing σ_R/σ_{tot} with 1/2. This modified bond-additivity model offers a marked improvement for molecules that are relatively thicker and retain significantly more than half of their "solvation area" after adsorption.

Acknowledgements

CTC acknowledges support of this work through the National Science Foundation under grant number CBET-2004757. NS and JA were sponsored by the Army Research Office and Army Research Laboratory (ARL) under Grant Number W911NF-21-1-0149. The views and conclusions contained in this document are those of the authors and should not be interpreted as representing the official policies, either expressed or implied, of the Army Research Office, Army Research Laboratory (ARL) or the U.S. Government. The U.S. Government is authorized

to reproduce and distribute reprints for Government purposes notwithstanding any copyright notation herein.

References

(1) Walker, T. W.; Chew, A. K.; Li, H.; Demir, B.; Zhang, Z. C.; Huber, G. W.; Van Lehn, R. C.; Dumesic, J. A. Universal Kinetic Solvent Effects in Acid-Catalyzed Reactions of Biomass-Derived Oxygenates. *Energy Environ. Sci.* **2018**, *11*, 617–628.

(2) Mellmer, M. A.; Sanpitakseree, C.; Demir, B.; Bai, P.; Ma, K.; Neurock, M.; Dumesic, J. A. Solvent-Enabled Control of Reactivity for Liquid-Phase Reactions of Biomass-Derived Compounds. *Nat. Catal.* **2018**, *1*, 199–207.

(3) Segal, E.; Madon, R. J.; Boudart, M. Catalytic Hydrogenation of Cyclohexene. I. Vapor-Phase Reaction on Supported Platinum. *J. Catal.* **1978**, *52*, 45–49.

(4) Madon, R. J.; O'Connell, J. P.; Boudart, M. Catalytic Hydrogenation of Cyclohexene: Part II. Liquid Phase Reaction on Supported Platinum in a Gradientless Slurry Reactor. *AIChE J.* **1978**, *24*, 904–911.

(5) Gonzo, E. E.; Boudart, M. Catalytic Hydrogenation of Cyclohexene. 3. Gas-Phase and Liquid-Phase Reaction on Supported Palladium. *J. Catal.* **1978**, *52*, 462–471.

(6) Qi, L.; Alamillo, R.; Elliott, W. A.; Andersen, A.; Hoyt, D. W.; Walter, E. D.; Han, K. S.; Washton, N. M.; Rioux, R. M.; Dumesic, J. A.; et al. Operando Solid-State NMR Observation of Solvent-Mediated Adsorption-Reaction of Carbohydrates in Zeolites. *ACS Catal.* **2017**, *7*, 3489–3500.

(7) He, J.; Liu, M.; Huang, K.; Walker, T. W.; Maravelias, C. T.; Dumesic, J. A.; Huber, G. W. Production of Levoglucosenone and 5-Hydroxymethylfurfural from Cellulose in Polar Aprotic Solvent-Water Mixtures. *Green Chem.* **2017**, *19*, 3642–3653.

(8) Mellmer, M. A.; Sener, C.; Gallo, J. M. R.; Luterbacher, J. S.; Alonso, D. M.; Dumesic, J. A. Solvent Effects in Acid-Catalyzed Biomass Conversion Reactions. *Angew. Chemie - Int. Ed.* **2014**, *53*, 11872–11875.

(9) Iyemperumal, S. K.; Deskins, N. A. Evaluating Solvent Effects at the Aqueous/Pt(111) Interface. *ChemPhysChem* **2017**, *18*, 2171–2190.

(10) Singh, N.; Sanyal, U.; Ruehl, G.; Stoerzinger, K. A.; Gutiérrez, O. Y.; Camaioni, D. M.; Fulton, J. L.; Lercher, J. A.; Campbell, C. T. Aqueous Phase Catalytic and Electrocatalytic Hydrogenation of Phenol and Benzaldehyde over Platinum Group Metals. *J. Catal.* **2020**, *382*, 372–384.

(11) Chen, F.; Shetty, M.; Wang, M.; Shi, H.; Liu, Y.; Camaioni, D. M.; Gutiérrez, O. Y.; Lercher, J. A. Differences in Mechanism and Rate of Zeolite-Catalyzed Cyclohexanol Dehydration in Apolar and Aqueous Phase. *ACS Catal.* **2021**, *11*, 2879–2888.

(12) Xie, T.; Bodenschatz, C. J.; Getman, R. B. Insights into the Roles of Water on the Aqueous Phase Reforming of Glycerol. *React. Chem. Eng.* **2019**, *4*, 383–392.

(13) Sheng, W.; Zhuang, Z.; Gao, M.; Zheng, J.; Chen, J. G.; Yan, Y. Correlating Hydrogen Oxidation and Evolution Activity on Platinum at Different pH with Measured Hydrogen Binding Energy. *Nat. Commun.* **2015**, *6*, 5848.

(14) Koch, G. H.; Brongers, M. P. H.; Thompson, N. G.; Virmani, Y. P.; Payer, J. H. *Corrosion Cost and Preventive Strategies in the United States*; 2002.

(15) Bockris, J. O.; Jeng, K. T. In-Situ Studies of Adsorption of Organic Compounds on Platinum Electrodes. *J. Electroanal. Chem.* **1992**, *330*, 541–581.

(16) Kristoffersen, H. H.; Shea, J.-E.; Metiu, H. Catechol and HCl Adsorption on TiO_2(110) in Vacuum and at the Water–TiO_2 Interface. *J. Phys. Chem. Lett.* **2015**, *6*, 2277–2281.

(17) Song, W.; Martsinovich, N.; Heckl, W. M.; Lackinger, M. Born-Haber Cycle for Monolayer Self-Assembly at the Liquid-Solid Interface: Assessing the Enthalpic Driving Force. *J. Am. Chem. Soc.* **2013**, *135*, 14854–14862.

(18) Yoon, Y.; Rousseau, R.; Weber, R. S.; Mei, D.; Lercher, J. A. First-Principles Study of Phenol Hydrogenation on Pt and Ni Catalysts in Aqueous Phase. *J. Am. Chem. Soc.* **2014**, *136*, 10287–10298.

(19) Singh, N.; Lee, M.-S.; Akhade, S. A.; Cheng, G.; Camaioni, D. M.; Gutiérrez, O. Y.; Glezakou, V.-A.; Rousseau, R.; Lercher, J. A.; Campbell, C. T. Impact of pH on Aqueous-Phase Phenol Hydrogenation Catalyzed by Carbon-Supported Pt and Rh. *ACS Catal.* **2019**, *9*, 1120–1128.

(20) Magnussen, O. M.; Groß, A. Toward an Atomic-Scale Understanding of Electrochemical Interface Structure and Dynamics. *J. Am. Chem. Soc.* **2019**, *141*, 4777–4790.

(21) Saleheen, M.; Heyden, A. Liquid-Phase Modeling in Heterogeneous Catalysis. *ACS Catal.* **2018**, *8*, 2188–2194.

(22) Zhang, X.; Sewell, T. E.; Glatz, B.; Sarupria, S.; Getman, R. B. On the Water Structure at Hydrophobic Interfaces and the Roles of Water on Transition-Metal Catalyzed Reactions: A Short Review. *Catal. Today* **2017**, *285*, 57–64.

(23) Zhang, X.; Defever, R. S.; Sarupria, S.; Getman, R. B. Free Energies of Catalytic Species Adsorbed to Pt(111) Surfaces under Liquid Solvent Calculated Using Classical and Quantum Approaches. *J. Chem. Inf. Model.* **2019**, *59*, 2190–2198.

(24) Granda-Marulanda, L. P.; Builes, S.; Koper, M. T. M.; Calle-Vallejo, F. Influence of Van Der Waals Interactions on the Solvation Energies of Adsorbates at Pt-Based Electrocatalysts. *ChemPhysChem* **2019**, *20*, 2968–2972.

(25) Schweitzer, B.; Steinmann, S. N.; Michel, C. Can Microsolvation Effects Be Estimated from Vacuum Computations? A Case-Study of Alcohol Decomposition at the H_2O/Pt(111) Interface. *Phys. Chem. Chem. Phys.* **2019**, *21*, 5368–5377.

(26) Klamt, A.; Schüürmann, G. COSMO: A New Approach to Dielectric Screening in Solvents with Explicit Expressions for the Screening Energy and Its Gradient. *J. Chem. Soc. Perkin Trans. 2* **1993**, *0*, 799–805.

(27) Zare, M.; Solomon, R. V.; Yang, W.; Yonge, A.; Heyden, A. Theoretical Investigation of Solvent Effects on the Hydrodeoxygenation of Propionic Acid over a Ni(111) Catalyst Model. *J. Phys. Chem. C* **2020**, *124*, 16488–16500.

(28) Gray, C. M.; Saravanan, K.; Wang, G.; Keith, J. A. Quantifying Solvation Energies at Solid/Liquid Interfaces Using Continuum Solvation Methods. *Mol. Simul.* **2017**, *43*, 420–427.

(29) Zhang, X.; Savara, A.; Getman, R. B. A Method for Obtaining Liquid-Solid Adsorption Rates from Molecular Dynamics Simulations: Applied to Methanol on Pt(111) in H_2O. *J. Chem. Theory Comput.* **2020**, *16*, 2680–2691.

(30) Yuk, S. F.; Lee, M.-S.; Akhade, S. A.; Nguyen, M.-T.; Glezakou, V.-A.; Rousseau, R. First-Principle Investigation on Catalytic Hydrogenation of Benzaldehyde over Pt-Group Metals. *Catal. Today* **2020**. https://doi.org/10.1016/j.cattod.2020.07.039.

(31) Clabaut, P.; Schweitzer, B.; Götz, A. W.; Michel, C.; Steinmann, S. N. Solvation Free Energies and Adsorption Energies at the Metal/Water Interface from Hybrid Quantum-Mechanical/Molecular Mechanics Simulations. *J. Chem. Theory Comput.* **2020**, *16*, 6539–6549.

(32) Singh, N.; Campbell, C. T. A Simple Bond-Additivity Model Explains Large Decreases in Heats of Adsorption in Solvents Versus Gas Phase: A Case Study with Phenol on Pt(111) in Water. *ACS Catal.* **2019**, *9*, 8116–8127.

(33) Rumptz, J. R.; Campbell, C. T. Adhesion Energies of Solvent Films to Pt(111) and Ni(111) Surfaces by Adsorption. *ACS Catal.* **2019**, *9*, 11819–11825.

(34) Gileadi, E. Electrosorption of Uncharged Molecules on Solid Electrodes. *J. Electroanal. Chem.* **1966**, *11*, 137–151.

(35) Akinola, J.; Barth, I.; Goldsmith, B. R.; Singh, N. Adsorption Energies of Oxygenated Aromatics and Organics on Rhodium and Platinum in Aqueous Phase. *ACS Catal.* **2020**, *10*, 4929–4941.

(36) Barone, V.; Cossi, M.; Tomasi, J. A New Definition of Cavities for the Computation of Solvation Free Energies by the Polarizable Continuum Model. *J. Chem. Phys.* **1997**, *107*, 3210–3221.

(37) Skyner, R. E.; McDonagh, J. L.; Groom, C. R.; Van Mourik, T.; Mitchell, J. B. O. A Review of Methods for the Calculation of Solution Free Energies and the Modelling of Systems in Solution. *Phys. Chem. Chem. Phys.* **2015**, *17*, 6174–6191.

(38) Carey, S. J.; Zhao, W.; Campbell, C. T. Energetics of Adsorbed Benzene on Ni(111) and Pt(111) by Calorimetry. *Surf. Sci.* **2018**, *676*, 9–16.

(39) Carey, S.; Zhao, W.; Mao, Z.; Campbell, C. T. Energetics of Adsorbed Phenol on Ni(111) and Pt(111) by Calorimetry. *J. Phys. Chem. C* **2019**, *123*, 7627–7632.

(40) Silbaugh, T. L.; Campbell, C. T. Energies of Formation Reactions Measured for Adsorbates on Late Transition Metal Surfaces. *J. Phys. Chem. C* **2016**, *120*, 25161–25172.

(41) Mantina, M.; Chamberlin, A. C.; Valero, R.; Cramer, C. J.; Truhlar, D. G. Consistent van Der Waals Radii for the Whole Main Group. *J. Phys. Chem. A* **2009**, *113*, 5806–5812.

(42) Guedes, R. C.; Coutinho, K.; Costa Cabrai, B. J.; Canuto, S.; Correia, C. F.; Borges dos Santos, R. M.; Martinho Simões, J. A. Solvent Effects on the Energetics of the Phenol O-H Bond: Differential Solvation of Phenol and Phenoxy Radical in Benzene and Acetonitrile. *J. Phys. Chem. A* **2003**, *107*, 9197–9207.

(43) Rumptz, J. R.; Campbell, C. T. Adhesion Energies of Liquid Hydrocarbon Solvents onto Pt(111), MgO(100), Graphene and TiO_2(110) from Temperature Programmed Desorption Energies. *J. Phys. Chem. C* (submitted).

(44) Kiselev, V. D.; Shakirova, I. I.; Potapova, L. N.; Kashaeva, H. A.; Kornilov, D. A. Heats of Solution of Liquid Solutes in Various Solvents. *Dataset Pap. Chem.* **2013**, 1–3.

(45) Adamson, A. W.; Gast, A. P. *Physical Chemistry of Surfaces*, 6th ed.; 1997.

(46) Singh, N.; Sanyal, U.; Fulton, J. L.; Gutiérrez, O. Y.; Lercher, J. A.; Campbell, C. T. Quantifying Adsorption of Organic Molecules on Platinum in Aqueous Phase by Hydrogen Site Blocking and In Situ X-Ray Absorption Spectroscopy. *ACS Catal.* **2019**, *9*, 6869–6881.

(47) Campbell, C. T.; Sellers, J. R. V. The Entropies of Adsorbed Molecules. *J. Am. Chem. Soc.* **2012**, *134*, 18109–18115.

(48) Lu, F.; Salaita, G. N.; Laguren-Davidson, L.; Stern, D. A.; Wellner, E.; Frank, D. G.; Batina, N.; Zapien, D. C.; Walton, N.; Hubbard, A. T. Characterization of Hydroquinone and Related Compounds Adsorbed at Pt(111) from Aqueous Solutions: Electron Energy-Loss Spectroscopy, Auger Spectroscopy, Low-Energy Electron Diffraction, and Cyclic Voltammetry. *Langmuir* **1988**, *4*, 637–646.

(49) Sander, R. Henry's Law Constants. In *NIST Chemistry WebBook, NIST Standard Reference Database Number 69, Eds. P.J. Linstrom and W.G. Mallard, National Institute of Standards and Technology, Gaithersburg MD, 20899*; 2018; pp 1–3.

(50) Israelachvili, J. N. *Intermolecular and Surface Forces*; Academic Press, 2011.

(51) Ketcham, W. M.; Hobbs, P. V. An Experimental Determination of the Surface Energies of Ice. *Philos. Mag.* **1969**, *19*, 1161–1173.

(52) Lew, W.; Crowe, M. C.; Karp, E.; Campbell, C. T. Energy of Molecularly Adsorbed Water on Clean Pt(111) and Pt(111) with Coadsorbed Oxygen by Calorimetry. *J. Phys. Chem. C* **2011**, *115*, 9164–9170.

(53) Pomerantz, P.; Clinton, W. C.; Zisman, W. A. Spreading Pressures and Coefficients, Interfacial Tensions, and Adhesion Energies of the Lower Alkanes, Alkenes, and Alkyl Benzenes on Water. *J. Colloid Interface Sci.* **1967**, *24*, 16–28.

(54) Campbell, C. T.; Mao, Z. Chemical Potential of Metal Atoms in Supported Nanoparticles: Dependence upon Particle Size and Support. *ACS Catal.* **2017**, *7*, 8460–8466.

TOC Graphic

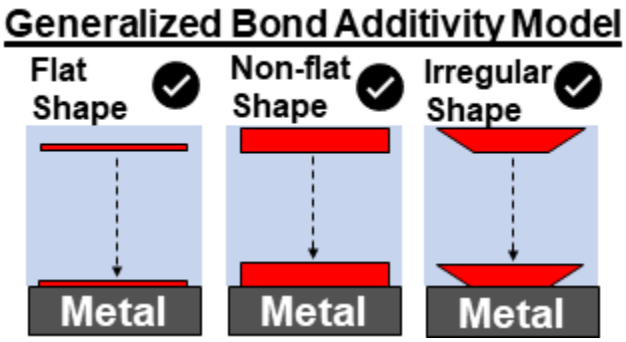
Generalized Bond Additivity Model
Flat Shape
Non-flat Shape
Irregular Shape
Metal
Metal
Metal